# Smart Sorption: Novel applications of cellulosic nanomaterials for selective critical metal recovery from black mass leachates through multibatch processes

Francisco de Borja Ojembarrena, Noemi Merayo, Angeles Blanco, Carlos Negro, Eric van Hullebusch

Separation and Purification Technology 341 (2024) 126940

Contents lists available at ScienceDirect

Separation and Purification Technology

journal homepage: www.elsevier.com/locate/seppur

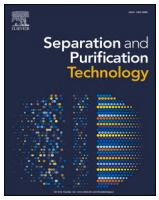

# Smart Sorption: Novel applications of cellulosic nanomaterials for selective critical metal recovery from black mass leachates through multibatch processes

Francisco de Borja Ojembarrena [a], Noemi Merayo [c], Angeles Blanco [a], Carlos Negro [a], Eric D. van Hullebusch [b,*]

[a] Cellulose, Paper and Advanced Water Treatments Research Group, Department of Chemical Engineering, Complutense University of Madrid, Avda. Complutense s/n, Madrid, Spain
[b] Université Paris Cité, Institut de Physique du Globe de Paris, CNRS, F-75005 Paris, France
[c] ETSIDI, Mechanical, Chemical and Industrial Design Eng. Dept., Universidad Politécnica de Madrid, Madrid, Spain

ARTICLE INFO

Editor: S. Deng

*Keywords:*
Critical metal recovery
Sorption
Black mass leaching
Cellulose nanocrystals
Cellulose nanofibers
Multiple step batch

ABSTRACT

Selective critical metal recovery from black mass leachates (BML) is a great challenge for the Li-ion batteries recycling sector. This paper shows the potential of nanocellulose products as green adsorbents for a selective recovery of critical metals through multibatch sorption processes. Cellulose nanocrystals (CNCs) and cellulose nanofibers (CNFs) of 0.4 and 1.5 meq/g cationic demand, respectively, have been produced and used as biosorbents. Metal leaching from non-pyrolyzed black mass with HCl presented the highest critical metal extraction yield, obtaining up to 10 g/L of Co and more than 1 g/L of Cu, Mn and Ni. The adsorbents were tested under different dosages and pH conditions for the treatment of both synthetic multimetal solution (MMS), with Mn, Cu, Co, and Ni, and real BML, through a multiple step batch treatment to increase the selectivity towards each critical metal. For MMS treatments, the lowest pH (1–2) conditions are favorable for Co separation, reaching 135 g/g, while higher pH values (4–5) are better to recover Cu and Ni. Selectivity indexes between metals could reached values above 40 for the optimal conditions. For the treatment of BML, pH around 3 enhanced the selectivity of Al and pH of 5 of the Li. In this case, metal recoveries were higher than 30 g/g. When CNCs were used, more than 4 g/g of Co was adsorbed, recovering more than 99 % of the Co present in the waste. 99 % of Co purity was obtained at the optimal Co selective recovery conditions. Although the studied critical metals were strongly sorbed onto the nanocelluloses, a solution with a concentration of 2.5–5 g/L of these metals could be extracted from desorption tests.

## 1. Introduction

In the last years, a rising interest in the recovery of valuable by-products from electronic waste has emerged. The recovery of critical metals through the application of recycling methods is becoming a priority due to the lack of natural resources. In the case of cities, governments are trying to exploit the potential of urban mining to achieve the goals of circular economy and urban sustainability. This factor is equally essential for the sustainability of companies that use them as raw materials, just like the battery, metal plating, or the electronic sectors. Circular economy, including material recyclability, minimization of waste production or revalorization of products in their end-of-life (EOL) stage has become one of the most relevant tendencies in research during the last two decades [1]. In the European Union (EU), the Directorate-General for Internal Market, Industry, Entrepreneurship and SMEs elaborates a List of Critical Raw Materials (CRMs) every 3 years since 2010. This List of CRMs is ruled by the EU Regulations 168/2013, 2018/858, 2018/1724 and 2019/1020 [2], and it is the official report which includes the state-of-the-art about the CRM and the list of new critical materials established by the European Union for the next period [3]. In

*Abbreviations:* BML, Black Mass Leachate; CC, Carboxylic Content; CD, Cationic Demand; CNCs, Cellulose Nanocrystals; CNFs, Cellulose Nanofibers; CRMs, Critical Raw Materials; EOL, End-of-Life; LIBs, Lithium-Ion Batteries; MMS, Multimetal Solution; MSB, Multiple Step Batch; NCs, Nanocelluloses; PDADMAC, Poly(diallyldimethylammonium chloride); PesNa, Polyethylenesulfonate; $T_{\lambda 600\ nm}$, Transmittance at λ=600 nm.

* Corresponding author.
*E-mail address:* vanhullebusch@ipgp.fr (E.D. van Hullebusch).

https://doi.org/10.1016/j.seppur.2024.126940
Received 10 December 2023; Received in revised form 30 January 2024; Accepted 27 February 2024
Available online 1 March 2024

2023, this list included several metals, such as cobalt, copper, nickel or manganese [3]. In the special case of cobalt and manganese, the reliance of EU on imports (81 % and 96 %, respectively) represents a critical risk of high relevance since their recycling rate from EOL products is low (22 % and 9 %, respectively) [3]. In the same way, the US Geological Survey (USGS) has proposed the 2022 List of Critical Minerals, where cobalt, manganese and nickel are also included [4]. According to the USGS, the US Government will focus the effort on assuring the maintenance of the supply chain of these critical metals, together with the rest of the minerals in the list [4]. In accordance to the OECD Trade Policy Paper on the CRM for the Green Transition, one of the main factors promoting the metal recyclability efforts in government policies is that the top 3 producers of the mentioned metals in 2019 reach up to a 50 % of the Cu and Ni production and reserves, a 55 % of Mn ones and a 75 % of the Co ones [5]. As an example of the relevance of this matter for certain regions, neither of those top 3 suppliers are EU members [5]. Thus, the rest of the zones must adapt their strategies on boosting the recyclability of this metals.

The recycling process of lithium ion spent batteries (LIBs) is composed of varied operations. These operations can be sorted as pretreatments like dismantling through mechanical treatments, as crushing, grinding, and sieving [6,7]. The final product obtained from the pretreatment is called black mass [6]. These black masses contain a large concentration of varied critical metals, such as cobalt, manganese or nickel [8]. In the last years, the interest on the recovery of these critical metals from spent LIBs has increased exponentially [9]. According to Google patents, the yearly number of patents dealing with “black mass metal recovery” has suffered a 9-fold rise between the 1990 s to the 2020 s, reaching around 22,500 patents per year [10]. Between the different technologies available for the metal recovery, hydrometallurgical and pyrometallurgical processes are the most developed and widely applied at industrial scale [11]. Pyrometallurgy allows the recovery of the metals without intense pretreatment, as the metals are recovered as an alloy which contains the high-added value metals present in the initial battery [11]. Although it is a well-known and efficient technology, this process is energy intensive and supposes a high operation cost, especially when a high grade of the metals (like copper or precious metals) is required [12]. Hydrometallurgical processes are a great alternative to the thermal processes. They are based on the leaching of the metals by applying solvents to the black mass after the application of the corresponding pretreatment [12]. Inorganic acids like HCl or $H_2SO_4$ have been widely applied for metal extraction [13]. These acids permit the obtention of high extraction yields from the black masses, even recovering more than 99 % of several metals [13]. The optimization of the operating conditions like solid–liquid ratio, acid selection or the presence of black mass pretreatment, is critical to reach the highest extraction of the metals [14].

The following step after metals leaching is the separation of the metals from the black mass leachate (BML) for their recovery. Several operations are available nowadays with this aim: solvent extraction, precipitation, ion exchange, electrochemical deposition, electrowinning or sorption [13,15,16]. Among them, sorption processes are an attractive choice for the recovery of metals, as they are inexpensive, simple to manage, and could be applied to several types of metals after an adequate optimization [15]. Generally, sorbents are applied in the treatment of effluents with low metal concentrations to comply with the limits of discharge [17]. In these cases, due to such low metal content, most of the highest sorption capacities of the metals reported in bibliography vary from dozens to a few hundred of mg of recovered metal per gram of adsorbent. These levels have been reported for the recovery of many metals, like cobalt [18,19], nickel [17], copper [17,20], neodymium [21] and gold [17], among others. On the other hand, the optimization of sorption processes to reach larger sorption capacities while introducing highly concentrated leachates is yet to be explored. A deeper investigation in the use of novel nanomaterials is necessary in the search of more efficient sorbents. Nanocellulose (NC) products have recently attracted the interest of researchers due to their promising behavior. These are nano-sized cellulosic materials which present a high surface area and a high number of active sites which surface can be easily modified [22]. There properties are essential to obtain large sorption capacities, high selectivity and strong binding affinity with the metals [23]. These NC sorbents can be made of sustainable and cost-effective lignocellulosic raw materials, whose production process viability is equally relevant to assess [23]. Two main different NC products can be produced from cellulosic sources: cellulose nanocrystals (CNCs) and cellulose nanofibers (CNFs) [24]. In the recent days, most of the applications of NC for metal sorption are dedicated to wastewater treatments, with the aim of substituting conventional sorbents like activated carbons by biosorbents [25,26]. Thus, their application in the recovery of critical metals from BML could imply a relevant advance for the further development of NC environmental applications although it has not been deeply studied yet.

Another important issue dealing with achieving high metal recovery yields is the selection of the operating conditions of the process. Commonly, published studies include experiments to adequate parameters as pH, sorbent dose or contact times. Nevertheless, the use of single batch experiments is abundant. Thus, the selection of other types of operation is usually not performed although it could provide useful data for a further implementation of the sorption process. With a view on this fact, one option to promote a larger and selective recovery of the metals could be a multiple step batch (MSB) operation. This operation has several advantages for the proposed objective of recovering metals from BML [27]. Thanks to the sequencing of the process into a certain number of cycles, it is easier to focus each step on the segregated recovery of the metals from BML. This would be performed through the application of the most critical optimized parameters for the sorption of each metal, like the type of NC, the dosing of sorbent and the operation pH.

The main objective of the present study is to design strategies based on multiple step batch sorption processes for the selective recovery of metals from BML by using NC products as sustainable sorbents. Thus, firstly BML are generated through the application of HCl and $H_2SO_4$ and CNCs and CNFs are synthesized and characterized. Secondly, the biosorbents are tested under different conditions for the removal of Mn, Cu, Co and Ni and the process is optimized for the selective removal of metals. Finally, desorption tests from spent CNCs and CNFs with different reagents are also carried out.

## 2. Materials and methods

### 2.1. Reagents and materials

The black masses used in this study were kindly supplied by a company dealing with Li-ion batteries recycling. There were two different types of black masses studied for the leaching tests, depending on the implementation of pyrolysis step to remove graphite from the black mass prior the acidic leaching.

The cellulosic sources to produce the CNFs and CNCs were bleached pulp from eucalyptus and commercial cotton linters, respectively, CNFs is produced by a TEMPO mediated oxidation and CNCs following an acid hydrolysis synthesis the procedures has been previously described by Ojembarrena et al. [28,29].

The commercial chemicals and solutions used in the experiments were: HCl (37 % v/v) and $H_2SO_4$ (98 % v/v), purchased from Labkem (Spain); hydroxylamine hydrochloride, 2,2,6,6-tetramethylpiperidin-1-yl-oxyl (TEMPO) and $AgNO_3$, purchased from Sigma Aldrich (USA); NaOH pellets, NaCl, NaBr and NaClO solution (10 % w/v), purchased from Panreac (Spain); $CuCl_2{\cdot}2\ H_2O$ and $CoCl_2{\cdot}6\ H_2O$, purchased from Fisher Scientific (USA); $MnCl_2{\cdot}4\ H_2O$ and $NiCl_2{\cdot}6\ H_2O$, purchased from Carlo Erba (Switzerland). The standard solutions of 0.001 N of poly (diallyldimethylammonium chloride) (PDADMAC) and polyethylenesulfonate (PesNA) used to determine the cationic demand were purchased from BTG Instruments AB (Sweden). The standard solutions

of Co, Mn, Cu, Ni, Fe, Zn, Al and Li (1.000 mg/mL) used to prepare the solutions for the calibration of the ICP device were purchased from Sigma Aldrich (USA). All the purchased reagents were of analytical grade. Dialysis membranes (12000–14000 Da weight cut-off) were necessary to purge the excess of acid during the CNC synthesis. The water used in all the experimental procedures was ultrapure water.

### 2.2. Synthesis routes of nanocellulose products

#### 2.2.1. Cellulose nanocrystals synthesis

The synthesis of CNCs was performed as indicated by Campano et al. (2020) [30]. In summary, the process is composed of a first acid hydrolysis of cotton linters and the following purification of the CNCs. The hydrolysis was carried out under mild heating (45 °C) and 64 % $H_2SO_4$ conditions. After 45 min, the slurry was diluted ten times and left settling overnight. The settled solids, which are the produced nanocrystals, were separated from the liquid. The purification process began with several cycles of washing and centrifuge of the samples to separate the acid excess from the CNCs. The end of this step happened once the supernatant presented turbidity, indicating that the isoelectric point of the CNCs was reached. To complete the removal of the excess of acid, the suspension was introduced into dialysis membranes and these membranes were immersed into water. When the pH descended, the added water gets replaced by pure water. This step is reproduced until a stable pH was reached. To finish the purification, the suspension gets homogenized by ultrasounds.

#### 2.2.2. Cellulose nanofibers synthesis

The CNFs were synthesized following the route established by Sanchez-Salvador et al. (2021) [31]. At first, a 1 % w/w suspension was produced by disintegrating the bleached pulp dispersed in water. The next step was the TEMPO-catalyzed reaction, which took place in a stirred beaker. The suspension was introduced into the beaker with TEMPO (0.1 mmol/g), NaBr (1 mmol/g) and a certain dose of NaClO. The applied doses of NaClO were 5 and 15 mmol/g, giving two different types of CNFs, called from now CNFs-5 and CNFs-15, respectively. The reaction lasted up to 120 min and the pH was kept stable at pH 10 through NaOH addition. Once finished, the TEMPO-oxidized CNFs were separated from the bulk and washed thoroughly to remove the impurities. After washing, the CNFs-5 and CNFs-15 were suspended again with water up to 1 % of consistency. The last part consisted of a homogenization process through a high-pressure homogenizer. This operation was performed in three sequential cycles at 600 bars of pressure. The homogenized suspensions were kept at 4 °C in the fridge until use.

### 2.3. Characterization of the nanocelluloses

The characterization of the synthetized CNF and CNC products was carried out considering their common properties. The consistency (%) of the synthetized nanocellulosic suspensions was calculated from the sample concentration (g/L). This parameter corresponds to the solid ratio of a nanocellulose suspension after a 24-h drying under 60 °C of temperature [32]. The cationic demand (CD) was measured through titration by adding PDADMAC to NCs suspensions of 0.1 % of consistency with an automatic titrator, as indicated by Balea et al. (2017) [33]. The transmittance at 600 nm ($T_{\lambda=600\ nm}$) of the 1:10 diluted CNFs suspensions through spectrophotometry was performed exactly as established by Serra-Parareda et al. (2021) [34]. The carboxylic content (CC) of the CNFs was determined through the conductimetric titration by following the procedure of Sanchez-Salvador et al. (2020) [35]. A suspension of 1.25 mg CNFs per mL of water with total of 0.8 mM of NaCl was titrated. The pH of the solution was firstly adjusted to 2.5–2.8 and kept in these levels with a NaOH solution 0.05 N during the titration. Finally, the production yield of the CNCs was evaluated as explained by Campano et al. (2020) [30].

### 2.4. Methodology applied for the acid leaching of pyrolyzed and non-pyrolyzed black masses

The pyrolyzed and non-pyrolyzed black masses were treated through hydrometallurgical processes with HCl and $H_2SO_4$. A literature survey was performed to evaluate the most adequate operating conditions for the acid leaching. The most relevant results are shown in Table S1 of the supplementary materials. This analysis showed that operating under solid:liquid ratios (S/L) of around 1:10, contact times between 60 and 180 min and acid dosage equivalent to 2 to 6 M of $H^+$ concentrations were adequate to leachate large concentrations of metals from LIBs waste. Thus, the selected operating conditions for the hydrometallurgical treatment of the black masses were S/L of 1:10, a contact time of 90 min and an acid dosage equivalent to 4 M of $H^+$ concentrations. All the experiments were carried out at room temperature. The experimental procedure was conducted for both pyrolyzed and non-pyrolyzed black masses as follows. Firstly, a dosage of 1 g of the selected black mass per 10 mL of acid (S/L equal to 1:10) were added to plastic tubes filled with 50 mL of volume. After a first quick stirring for some seconds under vortex agitation, the tubes were then placed onto the roller device. After 90 min of contact time, the content was centrifuged, and the leachate was separated from the black mass.

The metal content was measured through Inductively Coupled Plasma couples to optical emission spectrometry (ICP-OES). The measured samples were initially taken from the supernatant obtained from the centrifugation and filtered through syringe filters (0.22 μm of pore size). The filtered samples were then diluted with distilled $HNO_3$ 2 % v/v. After that, the tubes with the prepared samples were placed into the automatic sampler ready to be measured in the spectrometer. They were analyzed using a Spectrogreen spectrometer (Germany) applying a quartz nebulizer with a controlled flowrate passing through of 1 mL/min. This device was previously calibrated using dilutions of the standard solutions between 100 μg/L up to 50 mg/L. The analyses were triplicated for each sample.

### 2.5. Experimental multiple step batch treatment process for individual metal sorption onto cellulose nanocrystals and nanofibers

The treatment process for the selective metal recovery was designed based on the results previously obtained by optimizing the sorption of each metal onto each NC from individual metal solutions. To establish a comparison, a multiple metal solution (MMS) was prepared with the same concentration of the four metal cations (Co(II), Mn(II), Cu(II) and Ni(II)) as the treated BML.

#### 2.5.1. Development of a selective metal recovery process from synthetic multimetal solution or real black mass leachate

The designed treatment to recover the different metals from MMS or BML samples is presented in Fig. 1. In this process, a gradual increase of the pH between steps was performed. The starting pH is extremely low (approximately −0.6) due to the high concentration of the added HCl or $H_2SO_4$ to extract the metals from the black mass. The pH of the first treatment was risen to 1 and then increases in steps until reaching a pH of 5. The strategy of each step is explained below. An explanation on the selection of the conditions can be observed in Annex 2.

- Step 1: 5-step batches at pH 1 with CNCs (10 mg/L). Target metal: Co (II)
- Step 2: 3-step batches at pH 2 with CNFs-5 (15 mg/L). Target metal: Mn(II)
- Step 3: One-step batches at pH 3 with CNFs-5 (50 mg/L). Target metal: Cu(II)
- Step 4: 5-step batches at pH 3 with CNCs (10 mg/L). Target metal: Co (II)
- Step 5: 3-step batches at pH 4 with CNFs-15 (20 mg/L). Target metal: Co(II) and Ni(II)

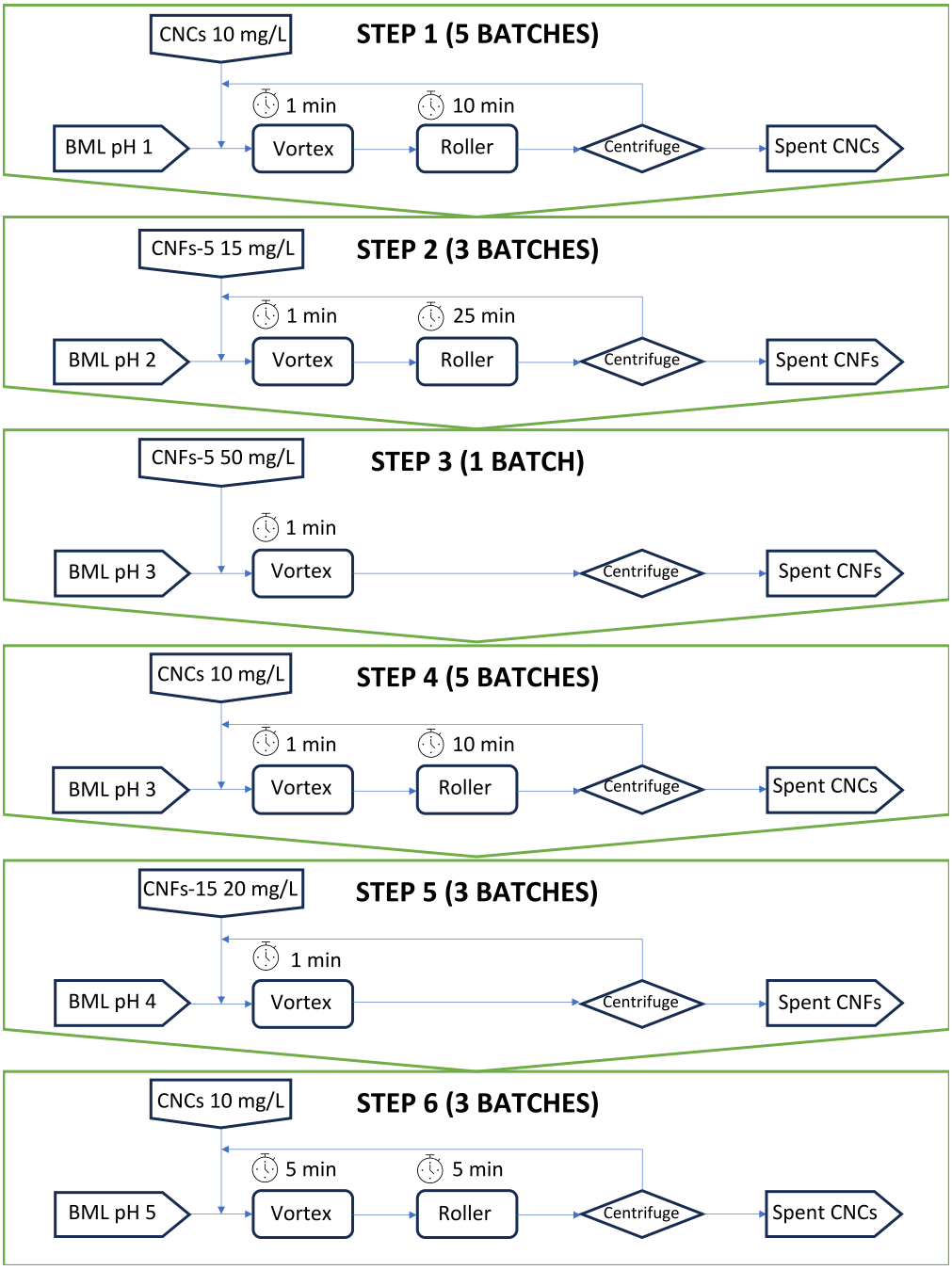


**Fig. 1.** BML or MMS treatment for selective recovery.

- Step 6: 3-step batches at pH 5 with CNCs (10 mg/L). Target metal: Ni (II)

The scheme of the MSB process also includes the applied stirring methods and the contact times. To separate the NCs from the liquid, a centrifugation step of 5 min at 4200 x g was needed, except for the step 3, where 15 min of centrifugation at 4200 x g were required due to the larger dosing. The total volume of the treated samples was 50 mL, and the pH was carefully controlled between each step batch with HCl and NaOH solutions. Small volume samples of the supernatant obtained from the centrifugation were taken in the end of each batch. The metal content of those samples was measured by ICP-OES following the procedure explained before. The metal content between batches was then measured to evaluate the metal recovery reached by the NCs. To differentiate the results between the batches, each one was named after its corresponding step and batch number. As an example, while talking about the batch number one of the first step, that batch would be named 1.1. This nomenclature will be applied during the whole paper. The metal recovery in each batch was calculated as indicated in eq. (1) and (2). Considering the initial concentration at each step and the recovery of each metal, selectivity was calculated as indicated in eq. (3).

$$NCrealmass[gdriedNC] = DosedNCmass[gsuspension]\hat{A}\cdot NCconsistency[\%] \quad (1)$$

$$Metalrecovery\left[\frac{mgmetal}{gNC}\right] = \frac{([Metal]_{Ini} - [Metal]_{Final})[mg/L]}{NCmass[gdriedNC]}\hat{A}\cdot V_{Treated}[L] \quad (2)$$

$$S_{Metal\ 1\ /\ Metal\ 2}\left[\frac{\left(\frac{mg\ sorbed\ M1}{mg\ initial\ M1}\right)}{\left(\frac{mg\ sorbed\ M2}{mg\ initial\ M2}\right)}\right] = \frac{(q_1[mg\ sorbed\ M1/g]/C_{Ini,\ 1}[mg\ initial\ M1/L])}{(q_2[mg\ sorbed\ M2/g]/C_{Ini,2}[mg\ initial\ M2/L])} \quad (3)$$

In Results and discussion section, the metal recovery yields reached while applying the MSB treatment to MMS will be discussed at first (Section 3.3.). Afterwards, BML treatment with NCs will be analyzed (Section 3.4.).

### 2.5.2. Optimization of the process for a maximum recovery of cobalt from real black mass leachate

Once confirmed that the concentration of cobalt in the BML was much higher than the rest of the analyzed metals, another process has been developed to maximize the specific recovery of Co, in all the steps.

Fig. 2 summarizes the experimental conditions of agitation and contact times applied in each step. As in the previous case, the centrifugation under the treatment of smaller sorbent doses (10 mg/L) was carried out during 5 min at 4200 x g, while at high dosages, a 15 min centrifugation at 4200 x g was needed to allow a better separation of the supernatant. The concentration of the metals was measured through ICP-OES The metal recovery of each batch was calculated according to eq. (1) and (2).

## 2.6. Metal desorption experiments

The metal desorption from the spent NC products was tested using different reagents, according to the state of the art. Diluted nitric and formic acids, and low-concentrated $NaNO_3$ solutions were capable to extract some of the studied metals, like Co(II) or Ni(II) [36–38]. The final selected solutions in accordance with the observed results in bibliography were $HNO_3$ 0.05 M; formic acid 0.5 M; and $NaNO_3$ 0.25 M. Ultrapure water was also tested as desorption reagent to allow the comparison of the results.

To perform these experiments, a batch for high metal recovery was performed under pH 4 at 10 mg/L of CNFs-15 dose. Then, the obtained CNFs-15 was divided into tubes filled with 0.2 g of wet spent CNFs-15, and a volume of 200 µL of each selected desorption reagent was added to each tube. A first vortex stirring for 5 min was applied to each tube to mix the suspension and after that, the tubes were placed on the roller for 90 min. After that, 1 mL of ultrapure water was added to each tube. This addition was necessary for the next step, as it permitted the pass of the samples through the 0.22 µm syringe filters. The sample was rapidly sucked and filtered from the tubes. The samples were then analyzed through ICP-OES. The desorption yield was calculated as indicated by eq. (4).

$$Desorptionyield[\%] = \frac{[Metal]_{Desorptionreagent}\left[\frac{mgmetal}{Lreagent}\right] \hat{A}\cdot V_{reagent}[L]}{Metalrecovery\left[\frac{mgmetal}{gNC}\right] \hat{A}\cdot DriedNCmass[gNC]} \hat{A}\cdot 100 \quad (4)$$

where the metal recovery and the dried mass of NC was calculated by using the eq. (1) and eq. (2).

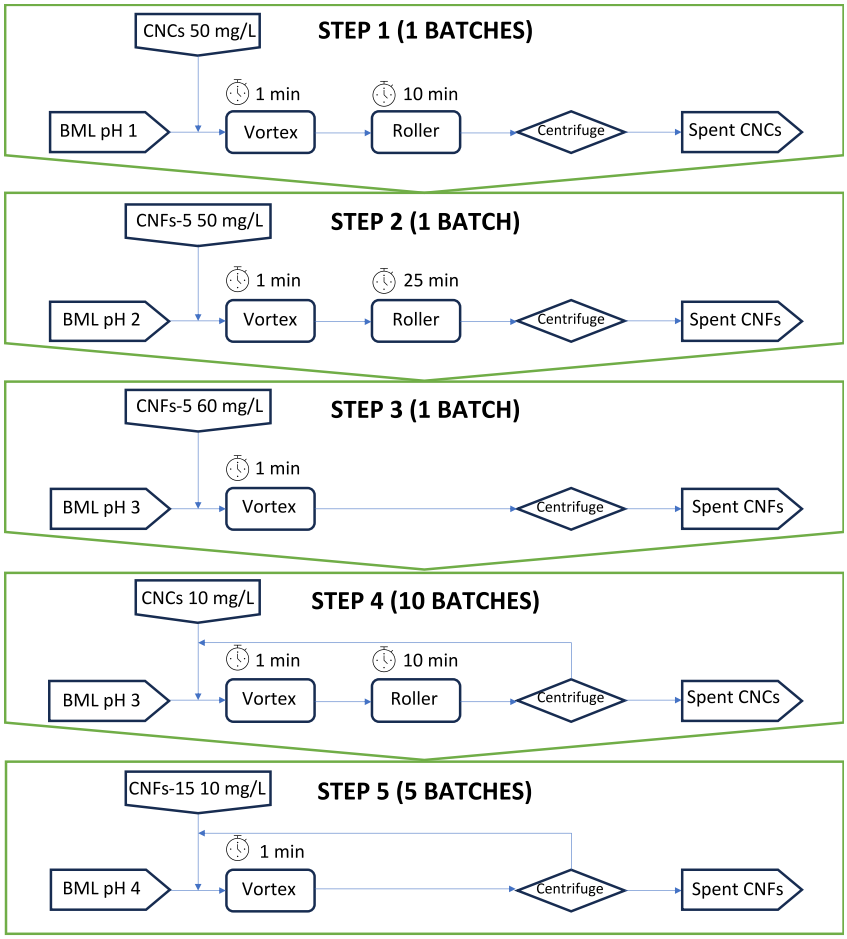


**Fig. 2.** Process definition for BML treatment for maximized Co recovery.

## 3. Results and discussion

### 3.1. Nanocellulose characterization

The characterization of the applied CNC, and TEMPO-CNFs was fully described in previous studies [28]. The consistencies of the synthetized CNCs, CNFs-5 and CNFs-15 corresponded to 0.43 ± 0.02 %; 1.11 ± 0.01 %; and 1.07 ± 0.01 % of dried NCs at 60 °C per mass unit of suspension. It is remarkable that all the synthetized materials reached high levels of active sites content, depicted by their high values of cationic demand, which varied between 0.40 meq/g, obtained in the case of the CNCs, to 1.55 and 1.72 meq/g in the cases of CNFs-5 and CNFs-15. A deep analysis on the TEMPO-oxidation kinetics of CNFs-5 was performed to evaluate the level of oxidation of the cellulosic material, which is proportional to the level of active sites revealed by the CD analysis. This evaluation is presented in Annex 3 of the supplementary material. The experimental kinetic data were fitted, and a continuous consumption of hypochlorite was observed until the end of the reaction after 100 min. In general terms, it can be stated that these materials present adequate properties to achieve a successful performance in the recovery of critical metals in extremely complex media, just like MMS or BML.

### 3.2. Acid leaching tests of black mass

The analyzed metal concentrations of the obtained leachates from the acid treatment of pyrolyzed (P) and non-pyrolyzed (NP) black masses can be seen in Fig. 3. Observing Fig. 3, it becomes clear that the differences between applying pyrolysis to the black mass or adding different types of acid was minor. In general terms, the order of magnitude of the concentration of the studied metals was similar with independence on the conditions. Co content was the highest of the analyzed metals in all the experiments, in accordance with other studies, such as Brückner et al. (2020) [39], who indicated that Co content could reach up to 33 % of total weight of $LiPF_6$ batteries; Widijatmoko et al. (2020) [40], who revealed that Co mass concentration was higher than 40 % in the fractions of black mass powder (<4750 μm of particle size); and Meshram et al. (2015) [41], whose study showed that Co mass fraction in cathode of LIBs was the highest one among the analyzed metals and was 3.1-fold larger than Mn, the second largest metal in the powder. The Co extraction yield was slightly increased when using NP black mass instead of the pyrolyzed one. The lowest Co content was reached by P BML with HCl (6.74 ± 0.24 g/L) and the maximum recorded concentration was 9.58 ± 0.02 g/L, achieved by HCl leaching of NP black mass. Mn and Li followed Co in the list of metal extraction. The $H_2SO_4$ NP BML reached much lower Mn levels (2.99 ± 0.01 g/L) than the other treatments, which varied from 3.53 ± 0.25 g/L to the 3.92 ± 0.01 g/L achieved during the NP black mass HCl leaching. Li content was equal in the case of P BML for both acids (3.95 g/L) but decreased for NP BML up to a 22 % for HCl and a 37 % for $H_2SO_4$. Al concentration varied between NP BML (around 2.2 g/L) and P BML (between 1.44 ± 0.04 g/L to 1.61 ± 0.06 g/L) but showed no influence on the type of acid applied. The concentrations of Ni followed the same trend as the Mn, reaching similar levels in all the cases (averaging 1.71 ± 0.07 g/L) except for $H_2SO_4$ NP black mass treatment. Cu leaching was lower than Ni, but its content was over 1 g/L in all the cases except the same case as Mn and Ni, where the extraction was much close to a half. In general terms, the leaching results of metals for the treatment with $H_2SO_4$ for NP black mass suffered a severe decay except for Co and Al. The leaching of Fe and Zn was around two orders of magnitude lower than the rest of the metals.

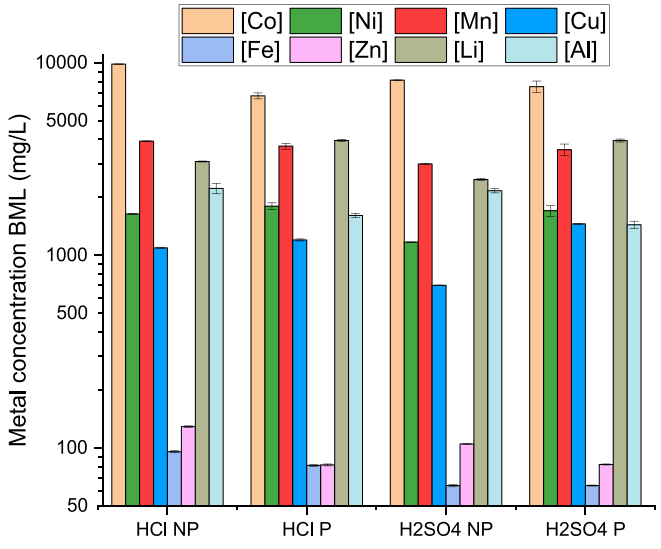


**Fig. 3.** ICP measurement of metal concentration after the acid leaching treatment of pyrolyzed (P) and non-pyrolyzed (NP) black mass through HCl (4 M) and $H_2SO_4$ (2 M). Operating conditions: 1:10 of S/L ratio, 90 min of contact time under roller stirring, and 50 mL of acid dosage.

The high leachability of the Co, Mn and Ni in highly concentrated HCl (up to 10 M) was recently explained by Balazs and Kekesi [42], who indicated that the predominant species of Mn and Co under 4 M of HCl concentration were really soluble, such as $Co^{2+}$, $CoCl^-$, $Mn^{2+}$ and $MnCl^-$; while only 1 % of the present Co and Mn species would be insoluble, like $CoCl_2$ or $MnCl_2$. These authors also presented a 1 M Pourbaix diagram of Ni, Mn and Co speciation against the reduction–oxidation potential ($E^0$ in V) and all of them presented only soluble species under pH values below zero (up to pH = -2) ($Co^{2+}$, $Ni^{2+}$ and $Mn^{2+}$) with redox potentials below 1.25 V [42]. As an idea, the redox potential of the HCl leachate of NP black mass was 0.95 V and extremely low pH below 0, which would involve that these divalent cations would be expected as predominant. In the case of Mn, the lower leaching under $H_2SO_4$ conditions while treating NP black mass could be explained by the results shown by Partinen et al. (2023) [43]. They reported a decay of Mn leaching while adding 1 M $H_2SO_4$ in the absence of chlorides due to the oxidation of $Mn^{2+}$ to $MnO_2$ at high temperatures and redox potential over 1.2 V [43]. In that case, the process would be favored by the larger amount of oxidizing reagent instead of the high temperatures. However, operating with P black mass higher extraction was achieved as the pyrolysis allows the formation of metal oxides of the transition metals, such as Ni or Mn, facilitating the acid leaching without further addition of any kind of aiding or oxidizing reagents [44].

After this experiment, the selected conditions to produce BML during the rest of the experiments was the application of HCl for NP black mass. The reason is that the generated BML contained a much larger Co concentration, which is important due to its high-added value metal, while similar levels of the other studied metals were obtained.

### 3.3. Application of the metal separation process to synthetic multimetal solution (MMS) treatment

The proposed treatment indicated in Fig. 1 was initially applied to the MMS sample produced by adding commercial metal chloride salts of the studied metals in the same level as the one measured in the BML. The results of mass of metal recovered and the percentage of recovery corresponding to each step can be seen in Fig. 4. As well, the total dosed dried NC and the overall metal recovery per mass unit of dosed NC achieved in the process could be observed in Table 1. The results indicate that Co recovery was higher than the rest of the metals, reaching 12.3 ± 2.1 g/g. Such values suppose an impressive level of recovery which has not been previously seen in bibliography. Most of the Co was recovered in the first step (up to 64 % of the total Co recovered). This MSB treatment with CNCs under pH 1 was also suitable for the recovery of Mn (67 %) and Ni (55 %). A large Mn uptake level was measured as well, up to 5.69 ± 0.93 g/g. Together with the first step, the step 4 (CNCs-multistep batches at pH 3) played an important role on the

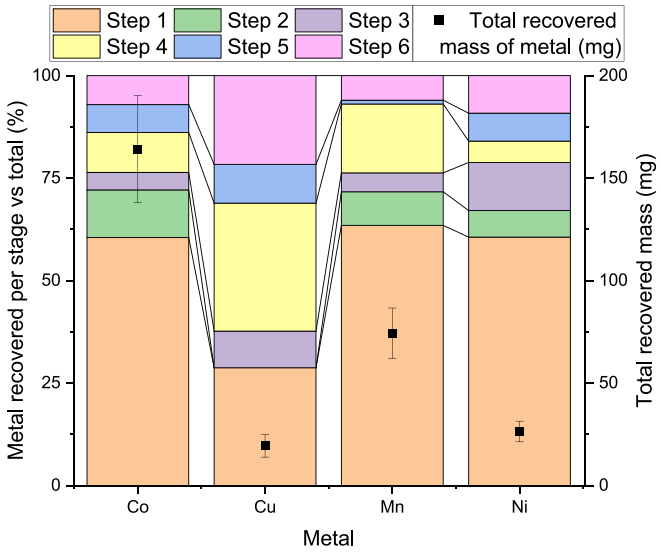


**Fig. 4.** Recovery yield per treatment step of Co, Cu, Mn, and Ni from MMS during the MSB treatment; and total metal recovery (total mg metal).

**Table 1**
Total dried NC dosed and overall metal recovery of Co, Cu, Mn, and Ni per mass unit of dosed NC during MSB treatment of MMS.

| Total dried NC dosage during MSB (mg NC) | Recovered metal | Overall metal recovery per mass unit of dosed NC (g/g) during MSB |
|---|---|---|
| 12.28 | Co | 12.30 ± 2.09 |
| | Cu | 1.58 ± 0.45 |
| | Mn | 5.69 ± 0.93 |
| | Ni | 2.38 ± 0.43 |

recovery of this metal, reaching up to the 18 % of the overall recovered Mn. Thus, the use of CNCs under acidic conditions (pH 1–3) seemed to be adequate for large Mn recoveries. Finally, the total metal recovery overpassed 1.5 g/g of metal recovery for Cu (1.58 ± 0.45 g/g) and Ni (2.38 ± 0.43 g/g). Cu could be recovered in similar levels in step 4 (31 % of the total Cu), step 1 (29 %), and step 6 (22 %). All these treatments were carried out by adding CNCs, which led to the fact that there is a good affinity between CNCs and Cu regardless the operating pH.

Considering the levels of metal recoveries, they exceeded the CD values of the materials in orders of magnitude, which indicates that other mechanisms must be involved in the removal beyond electrostatic attraction. In the case of Cu(II), the average recovery was up to 12 meq/g, while the CD values of the NC materials moved from 0.4 to 1.5 meq/g. These other mechanisms which play a considerable role in the metal separation were also observed and studied in the single metal solution tests with the NCs.

The evolution of the metal recoveries in every step, considering the performed batches, is shown in Fig. 5. There is a clear difference between Co and Mn trends (Fig. 5. a) and b)) and Cu and Ni (Fig. 5. c) and d)). Even though all the materials were mainly recovered in the first part of the first step treatment, there is a strong reduction in the Co recovery in the subsequent steps. Co recoveries were found to be up to 135.38 ± 7.00 g/g, 64.99 ± 5.64 g/g and 10.83 ± 5.20 g/g in the batches 1, 3 and 4 in step 1 (from now 1.1, 1.3 and 1.4, respectively); whereas 16.81 ± 6.51 g/g in the batch 2.1 and 10.11 ± 3.12 g/g in the batch 4.1 were achieved. Co supposed the totality of the recovered metal in the batch 2.3; and 81 % of the total metal recovery in the batch 5.1. The trend of Mn was similar, suffering a decay on the recovery as pH was increased between steps. Mn recovery became negligible in the fifth and sixth steps. The maximum recoveries of Mn were reached in the first step: 61.27 ± 4.39 g/g (step 1.1) and 43.51 ± 4.53 g/g (1.3). After that, only two of the batches reached values in the order of 10 g/g, which were 2.1 and 4.2. The 61 g/g Mn recovery value in the first step are higher of the ones obtained by Silva and Orefice [45] of 50 g/g through castor oil polyurethane foam containing cellulose-halloysite nanocomposite. The main difference was that in the case of the step 1.1 conditions, the concentration of Mn(II), and therefore, the driving force was up to 19-fold shorter than the applied by the mentioned authors. This shows the strong performance of the NC surfaces for metal attachment. On the other hand, Cu and Ni were mainly recovered in the very first batch of the experiment (1.1), where 7.18 ± 2.02 g/g and 21.02 ± 0.98 g/g were obtained. As well, the batch 1.3 was suitable to obtain close to 10 g/g of Ni uptake, and afterwards, during the steps 4 to 6 for Cu, and 5 to 6 for Ni, additional uptakes were achieved. This suggests that the attraction of these metals was enhanced by the increase of the pH to 3 and 4. This is better seen in the batch 4.2, (7.12 ± 1.81 g/g of Cu recovered) and in all the batches of step 6, where the levels of Cu and Ni recovery exceeded 4 and 6 g/g, respectively. Due to their lower concentrations, the purities of Cu and Ni were lower than the case of Mn and Co. Nevertheless, in the steps 6.1 and 6.3, a combination of approximately 60 % of Ni and 40 % of Cu was separated from the matrix.

The selectivity analysis indicated that in some intermediate batches, the selectivity was maximized towards some of the metals. The most relevant results of this analysis can be observed in Table S2. Those cases in which a metal presented a high selectivity did not meant that those metals reached the highest mass recovered. The high selectivity meant that such metal recovery was more prioritized than the rest of the metals even if its concentration was much lower. In any case, the achievement of extremely high selectivity values, allowing the enlarged recovery of each metal individually, is crucial. As an example, during the batch 2.3, it was revealed a maximized recovery of Co (with CNFs-5 at pH 2), which could be a good first treatment for Co recovery at the beginning of the process. The calculated selectivity towards Co against Mn were up to 32 recovery and the recoveries of Cu and Ni were not observed. Thus, 98.7 % of total metal recovery during that step corresponded to Co. The high values of Co recovery under low pH are not commonly seen in celluloses, mainly due to the low metal concentrations and high S/L ratios usually applied during the pH tests [46]. Those conditions cause the proton content to be strongly competitive against $Co^{2+}$ ions to be sorbed. In the case of step 1 conditions, the Co(II) concentration was up to 0.14 M, while the $H^+$ content was 0.09 M. Thus, the driving forces of both ions are in the same order of magnitude, reducing the selectivity towards $H^+$.

Afterwards, operating in batch 4.3 under higher pH conditions (pH 3) and adding CNFs-5, the maximization of the recovery of Mn was favored. The selectivity values, calculated according to eq. (3), against Co and Cu were 42.8 and 12.9, respectively, and Ni(II) was not recovered at all. Under the said conditions, up to 92.7 % of the total metal recovered in this step was Mn. The selectivity index values are in the order of the Mn(II)-Ni(II) (11) and Mn(II)–Co(II) (54) selectivities obtained by Silva and Orefice [45].

Cu and Ni were present in smaller concentrations, in the order of 1 g/L, which is around eight and four times lower than the Co and Mn contents. This suggests that they present a proportional reduction on the driving forces from the bulk to the NC surface. In practice, when pH was increased, the selectivity ratios of Ni and Cu compared to the rest were also risen, especially the Cu one. The best result was reached in step 6 (at pH 5 and through CNCs addition), mainly as a mixture 60:40 w/w of Ni and Cu was obtained, with low impurities of Co and Mn. This similar behavior of Ni(II) and Cu(II) with cellulosic materials at pH 4–6 was previously observed by Hokkanen et al., who indicated that Ni(II) was present as $Ni^{2+}$ while other cationic species from Cu(II) like $Cu_2OH_2^{2+}$, $Cu_3OH_4^{2+}$ and $CuOH^+$ were present as pH was risen, enhancing their removal [47].

Compared with bibliographic references, a recent study on the application of activated carbons with high sorption capacities (around 1.0–1.6 meq/g of active groups, next to the CNFs values) to the

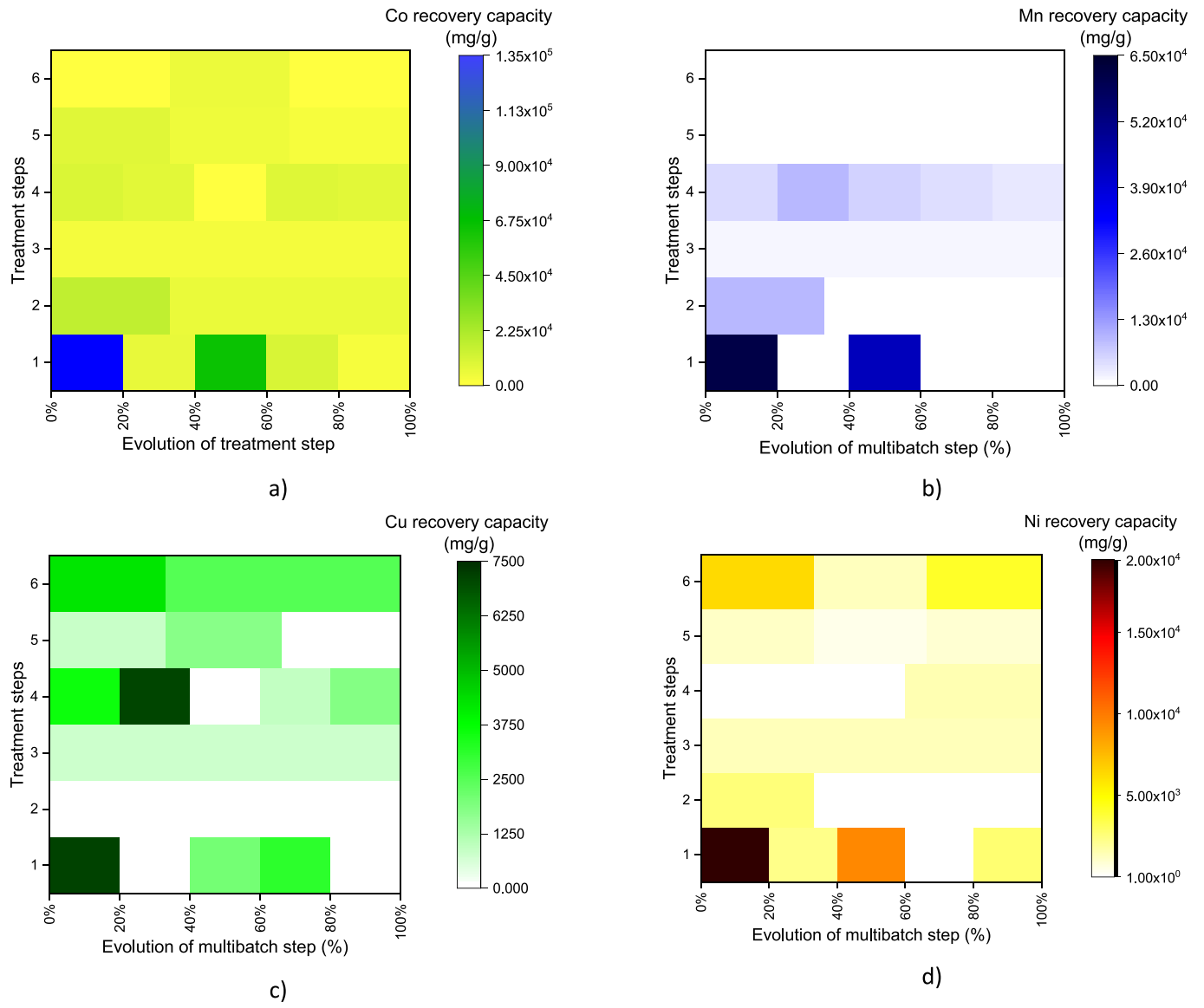


**Fig. 5.** Metal recovery evolution during the MSB treatments of MMS of a) Co; b) Mn; c) Cu; and d) Ni.

treatment of LIBs leachate revealed that, after applying previously optimized conditions, this material was only able to recover the mixed divalent metals (Ni(II), Mn(II) and Co(II)) with high selectivity against the lithium ion [48]. The authors of this study remarked the difficulty in the achievement of the separation of those divalent metals which are close one to another in the periodic table and show similar properties [48], showing the relevance of the results achieved through MSB.

### *3.4. Application of the metal separation process to real black mass leachate (BML)*

The BML obtained from HCl applied to NP black mass was used to assess the metal separation process. The process described on Fig. 1 was applied in the same way as for the MMS treatment. The results of masses of metal recoveries sorbed onto the NCs, and the percentage recovered in each step can be seen in Fig. 6. The results of recovery per unit of dosed dried NC was calculated. This result could be observed for the studied metals in Table 2. In general terms, the achieved recoveries of the metals were high, especially in the case of Co (7.34 ± 2.04 g/g). The Li, Al and Mn were recovered in the order of 2 g/g, while the values for Cu and Ni were found to be around 1 g/g. The results present a decay compared to the case of MMS without other competitors which varies from 41 % of Co to 60 % of Mn. This is caused to the presence of competing ions which could cover the active sites. This competition causes that a large amount of Al and Li fixed onto the NCs, in equivalent levels to the Mn uptake. The work recently performed by Fernando and Chavan [49] have tested EDTA-modified Zr-MOF-808 adsorbent to recover $Ni^{2+}$ from real citric acid black mass. The $Ni^{2+}$ recovery decayed a 50 % from 70 mg/g of $Ni^{2+}$ individual solutions to the treatment of the synthetic multimetal ($Ni^{2+}$, $Co^{2+}$, $Mn^{2+}$ and $Li^{+}$) solution. These authors revealed that non-observable recovery of $Ni^{2+}$ under optimized conditions was observed in the treatment of real BML [49]. Such levels of reducing efficiency after moving forward to more complex matrices reveals the relevance of the present study in maintaining large metal capacities onto the NCs even under treating real BML. Strauss et al. (2021) [50] also developed the treatment of real BML obtained by adding the black mass to $H_2SO_4$ 1 M and $FeSO_4$ 10 M through the application of Dowex ion-exchange resins. This method showed a maximum recovery of Co and Ni of 578 and 267 mg per bed volume before the column breakthrough was reached, equivalent to 43.13 mg/g and 19.94 mg/g, respectively [50]. These aforementioned capacities would confirm that the use of NC allows us the obtention of two orders of

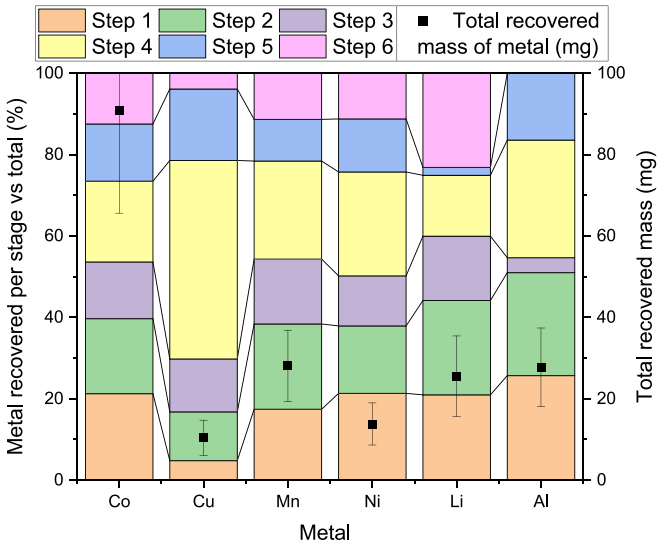


**Fig. 6.** Recovery yield per treatment step of Co, Cu, Mn, Ni, Li, and Al from real BML during the MSB treatment; and total metal recovery (mg metal per g of dosed NC).

**Table 2**
Total dried NC dosed and overall metal recovery of Co, Cu, Mn, Ni, Li, and Al per mass unit of dosed NC during MSB treatment of BML.

| Total dried NC dosage during MSB (mg NC) | Recovered metal | Metal recovery per mass unit of dosed NC (g/g) during MSB |
|---|---|---|
| 12.39 | Co | 7.34 ± 2.04 |
| | Cu | 0.84 ± 0.35 |
| | Mn | 2.27 ± 0.71 |
| | Ni | 1.11 ± 0.42 |
| | Li | 2.06 ± 0.80 |
| | Al | 2.24 ± 0.79 |

magnitude higher values of metal recovery than commonly used sorbents and ion-exchangers.

The analysis of the performance of the batches carried out in each step for each metal could be appreciated in Fig. 7. In the analysis of the metal recovery from the BML, it could be confirmed that the large metal recovery values over 10 g/g was only limited to Co recovery. This was mainly caused by the rise in the number of present ions competing against the studied ones, as could be observed by the large recoveries of Al and Li observed during the tests. Co was present in several samples, due to its high concentration, and this fact reduced the selectivity of other metals against this one. Most of the metals could be recovered at some batch in the tested steps, except for the Al in the step 6, whose high pH led to its precipitation as $Al(OH)_3$, avoiding its recovery regardless the batches applied. This factor was caused by the pH switch from pH 4, where the solubility of Al(III) was in the order of $10^{-2}$ M, to the pH 5 conditions, where its solubility decays to the order of $10^{-6}$ M [51]. Thus, at the Al(III) content ($3.7{\cdot}10^{-3}$ M) in this step, the homogeneous precipitation of Al(III) occurred. The generation of solid $Al(OH)_3$ attracted many metal ions to the surface, obtaining a precipitate which contained the 80 % of the Cu(II) present in solution, 22 % of the Ni(II), 20 % of the Co(II), and 10 % of the Mn(II), but leaving the soluble Li almost untouched. As a result, Li recovery was boosted in the step 6, thanks to the maintenance in the driving force while most of the recovery levels of other metals was sensibly lowered.

The results of selectivity were in the same way as for the MMS treatment. The calculated selectivity indexes are presented in Table S3 in the Supplementary Materials. In many steps it was found that the selectivity of the analyzed metal in each case was only high towards one of the other analyzed metals, but not to all of them. In fact, it was feasible to reach selectivity values over 2.0 of a single metal against all the rest studied metals only in the case of Al, in the batches 1.3, 4.4 and 5.3. Mn presented high capacities but normally, it showed the lowest affinity for NC against the rest, in terms of selectivity. This happened mainly after step 3, when pH values were 3 or above. The competition against Cu(II) was the main reason as the gradual generation of cationic Cu(II) species with lower charge increased their fixation to NCs. The increase in $Cu(OH)_2$ supported onto the material surfaces as pH is increased by surface precipitation and heterogeneous crystallization was observed in other materials like zeolites [52]. This also happened to Ni (II), which presented a surface precipitation of Ni onto hydroxyapatite-bentonite clay-CNCs composite even below the solubility values. This fact was caused by the presence of phosphates and silicates hydroxyapatite and bentonite which promoted the formation of crystals [53]. The Li and NC interaction was only enhanced in step 6 due to the decrease in the content of other metals caused by the $Al(OH)_3$ precipitation at pH 5. The product obtained during the step 6 could be really valuable for industry. The batches 6.1, 6.2 and 6.3 contained up to 8.90, 12.38 and 28.64 g/g of the metals of which lithium Manganese Nickel Cobalt Oxides (also known as LMNCO) batteries are composed of [54].

In the end, there were certain steps where maximum Al selectivity could be found. Li selectivity was enhanced after pH 5; and Co was present in most of the obtained samples, preferably in the lowest pH ones. The Cu and Ni mixtures with high purity obtained in MMS could not be reproduced in the complex BML due to the high presence of other metals, and Mn showed a relatively low affinity for the NCs compared to other soluble metals present in the BML.

### *3.5. Application of the metal separation process to real black mass leachate (BML) for maximum cobalt recovery*

After the analysis of the results provided by the BML treatment from the previous experiment, it was clear that the high content of Co would provoke its presence in most of the analyzed steps. Thus, a last process involving the maximization of Co recovery was attempted, following the steps indicated in Fig. 2. The mass of recovered metal during the analyzed process and the percentage of recovery corresponding to each step can be observed in Fig. 8. The metal recovery per mass unit is presented in Table 3. The recovery in the step 1 seemed clearly favorable to the sorption of Co onto the CNCs at pH 1, rather than the rest of the metals. The trend in total metal recovery of the rest of the metals looked in the same manner as the last experiment performed for BML treatment.

A deeper comparison between batches would reveal differences in the treatment results, where it would be shown that Co recovery could be enhanced. The analysis of the batches where the Co recovery was higher than the total recovery of the rest of the metals can be observed in Fig. 9. The spent NCs obtained after each batch could be observed in Figure S1. In the batches 1, 3, 4.4 and 4.5, almost all the metal recovery was associated to Co, and the mass ratio of recovered Co among total measured metal recovery was 99.2 %, 98.8 %, 93.7 % and 93.9 %, respectively. The high recovery obtained in these tests (4.34–7.94 g/g of Co) indicates that the obtained product would be useful for the final industry of wasted LIBs management. This can be demonstrated by the final aspect of NC after Co-recovery treatment in Figures S1. Such results are impressive and could be comparable to the selectivity values and mass ratios obtained through the use of Dowex ion exchange resins under optimized conditions applied by Strauss et al. [50]. While comparing this type of resins with CNCs and CNFs, it is also relevant to compare the costs. Although Merck indicates that the applied Dowex M4195 is a discontinued product, the pricing of other Merck cation exchange products (AmberSep, Dowex or AmberChrom) can be found around 200–500 US$/kg [55]. NCs materials synthetized in this paper from inexpensive raw materials, like eucalyptus bleached pulp (around 650 US$/ton in 2023) [56], in the case of CNCs and cotton linters (around 320 US$/ton in 2017. This data is comparable to the Q4 2023 price, as a similar COTLOOK A index value was observed in both

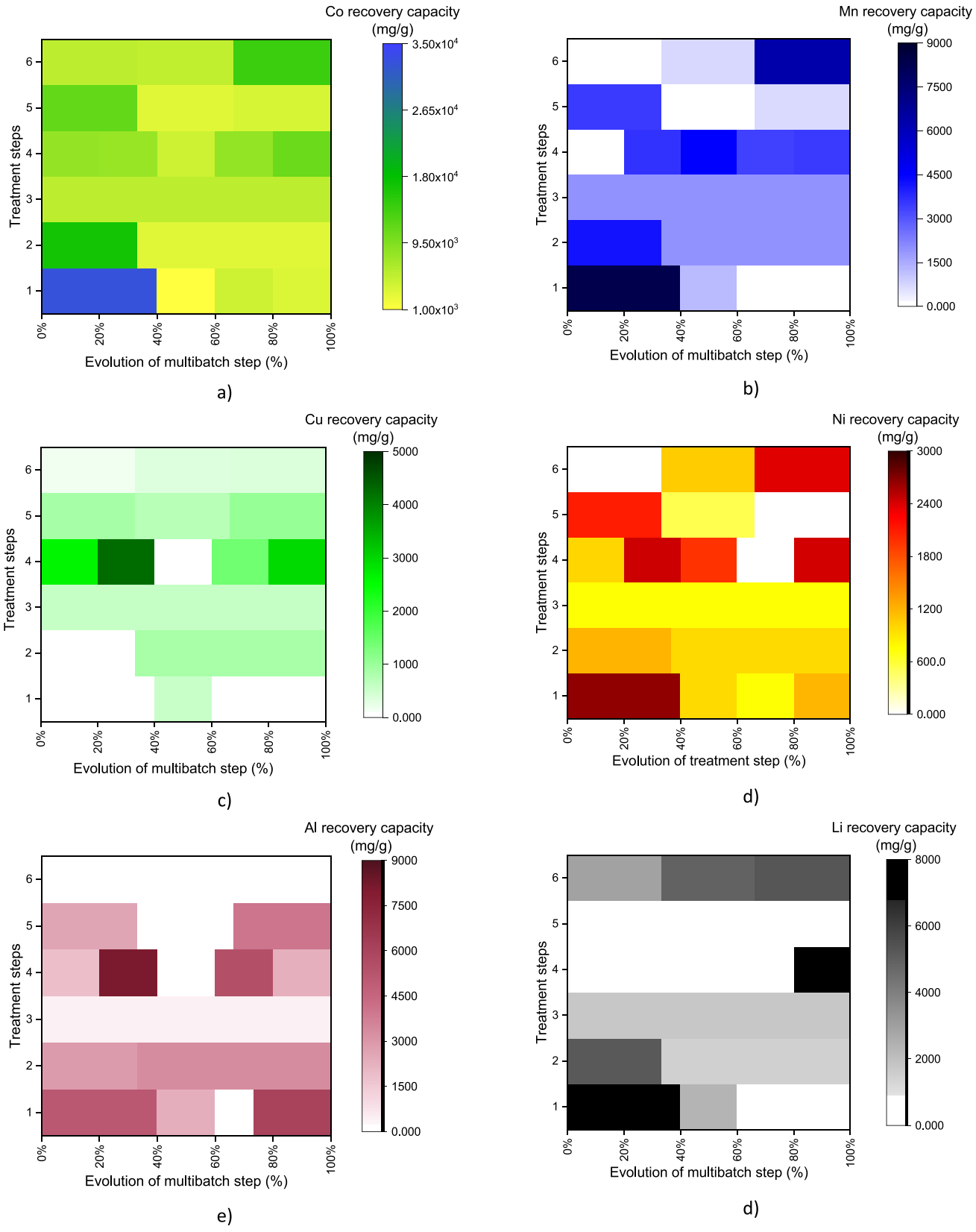


**Fig. 7.** Metal recovery evolution during the MSB treatments of real BML of a) Co; b) Ni; c) Cu; d) Ni; e) Al; and f) Li.

seasons, according to ICAC statistics, which provides similar cotton and cotton derivatives prices during both seasons) [57,58], in the case of CNFs. The most consumed chemical in the production of CNCs is $H_2SO_4$ (64 %), whose recovery in the process through microfiltration (up to 65 % of recovery yield) has been demonstrated in pilot scale [59]. Low-cost NaClO (5–15 mmol/g), and NaOH (around 2 mmol/g for pH control) are widely used for CNFs synthesis, as well as NaBr and TEMPO (1 and 0.1 mmol/g, respectively) as catalysts. Some authors have reached high

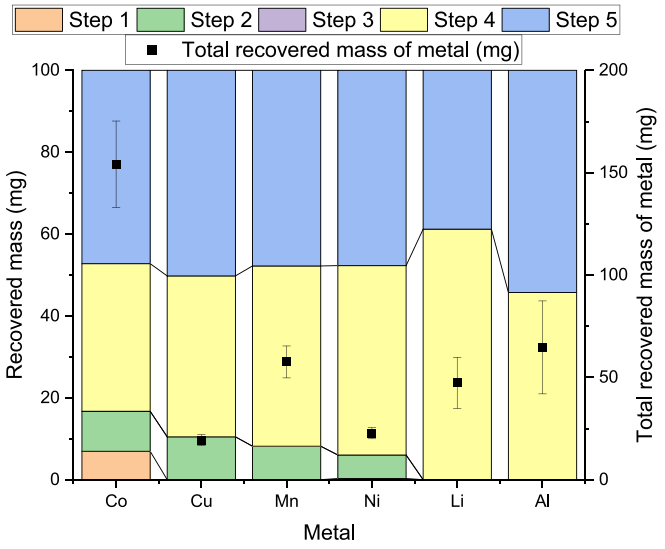


**Fig. 8.** Recovery yield per treatment step of Co, Cu, Mn, Ni, Li, and Al; from real BML during the MSB treatment for maximized Co recovery; and total metal recovery (mg metal per g of dosed NC).

**Table 3**
Total dried NC dosed and overall metal recovery of Co, Cu, Mn, Ni, Li, and Al per mass unit of dosed NC during MSB treatment of maximized recovery of Co.

| Total dried NC dosage during MSB (mg NC) | Recovered metal | Metal recovery per mass unit of dosed NC (g/g) during MSB |
|---|---|---|
| 16.05 | Co | 9.60 ± 1.31 |
| | Cu | 1.20 ± 0.17 |
| | Mn | 3.58 ± 0.48 |
| | Ni | 1.41 ± 0.17 |
| | Li | 2.95 ± 0.78 |
| | Al | 4.03 ± 1.42 |

efficiency in the recycling of reaction medium by separating it from the synthetized CNFs through filtration during several cycles [60,61]. These authors remarked that only a partial replacement of the spent oxidizing NaClO is needed between cycles, but not the most expensive chemicals (NaBr and TEMPO). Therefore, thanks to this reduced raw material costs, the tested CNCs and CNFs may become a real sustainable and competitive alternative to the nowadays solution of ion exchange resins. Similar cost-comparison studies between NCs and commercial materials for metal sorption for other industrial applications have been recently published [28].

In the step 4.3, almost no recovery of other metals was observed, except for Al. The selectivity level of Co towards Al was 1.49, which indicates a larger preference for Co. Nevertheless, the fact that a mixture of mainly two metals with a high recovery and mass ratio of Co (7.94 mg/g and 82.7 %, respectively) represent a good approach to obtain high added-value products for the industry. The last batch treatment with a high amount of Co onto the NC (up to 60 % of the total measured metal recovery) was batch 4.2. It presented one of the highest recoveries overall, but Co was mixed with similar amounts of Al, Li, and Mn. This mixture contains large amounts of valuable metals, although a probable posterior treatment of purification could be needed to add value to the final product.

Once observed the high purity obtained of Co in the analyzed stages, this process could be compared to other multiple step processes, like counter current solvent extraction. This type of process takes place in different batches, whose number is established by the equilibrium in each stage. They can be graphically calculated through McCabe-Thiele method [62]. This process is extremely efficient, specially under controlled conditions with certain solvents like Cyanex 242, D2EHPA or TBP [62–64]. Nevertheless, it shows some differences with the scheme of the present study. Firstly, most of the solvent extraction processes for Co require some BML treatments, like the pH adjustment above 4, normally 5–7; the saponification of the solvent with NaOH in some cases; and the previous recovery of other metals through precipitation or solvent extraction with other solvents [62–64]. In the presented MSB process, only NCs and low pH conditions, closer to the ones of the generated BML, were used to reach high Co recovery. This way of operation minimizes the operating costs of the MSB through sorption

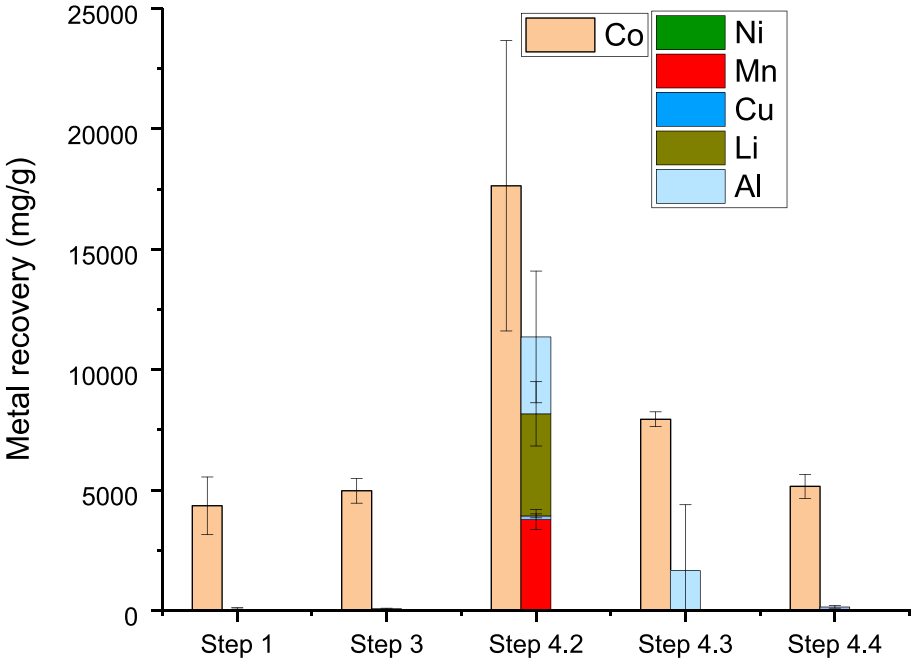


**Fig. 9.** Metal recovery of Co (single column) and other metals (Cu, Mn, Ni, Fe, Li and Al; stacked column) in the maximum Co selectivity steps during the BML treatment.

compared to solvent extraction. Other relevant difference is the required treatment volume. Both solvent extraction and sorption may take place in batches may be simply divided in BML feed, solvent or sorbent addition, mixing contact time and final separation of spent solvent (by phase separation) or sorbent (by settling) under low or inexistent stirring [63]. A typical organic-to-aqueous phase ratio could be 1:1 to 3:1 in solvent extraction, during contact times of 5 to 45 min (typically 10–20 min) [62–64]. In the sorption MSB process, the sorbent dosages applied in the process reach a maximum of 50 mg solid NC/L and the contact times are just one minute. This mainly involves that solvent extraction contactors would be much bigger due to the higher flowrates (2 to 4-times larger than the BML feed, compared to mainly the BML feed and the small volume of NCs in the sorption processes), and the much longer contact times. This would also mean a much higher energy cost associated to mixing and pumping in the case of solvent extraction per unit of volume of treated BML. As well, the short contact times required for NC sorption with BML, compared to solvent extraction, would facilitate the operation in single tanks in which a whole step (MSB and NC feed, one minute contact, settling, separation of NC, BML ready to receive fresh NC) may take place. This would reduce the capital costs and simplify the operation.

### 3.6. Results of desorption tests

The last test applied to the spent NC was the desorption process. The result of application of the different desorption solutions (ultrapure water, diluted $HNO_3$, formic acid or $NaNO_3$ solutions) is shown in Fig. 10. The presence of large concentrations of Co (4.5–5.1 g/L), Mn (1.9–2.1 g/L), Li (1.7–1.9 g/L), Ni (around 0.8 g/L) and Cu (around 0.6 g/L) was obtained with independence on the applied desorption reagent. The results obtained with $HNO_3$, formic acid and $NaNO_3$ were almost identical to the ones reflected in the application of ultrapure water. As an idea, the Co, Mn and Li desorbed level values after applying the desorption reagent in this experiment were three orders of magnitude above the values of Zn, Cd, Cu and Ni concentrations in $HNO_3$ (1 M) recovered from succinic acid mercerized nanocellulose [36]. They also exceeded in two orders of magnitude the desorbed As(V) concentration obtained in its recovery from polyethyleneimine-glutaraldehyde grafted CNCs by applying 0.1 M NaOH solution [65]. Compared to the values found in bibliography, similar results were reached by applying HCl 1 M

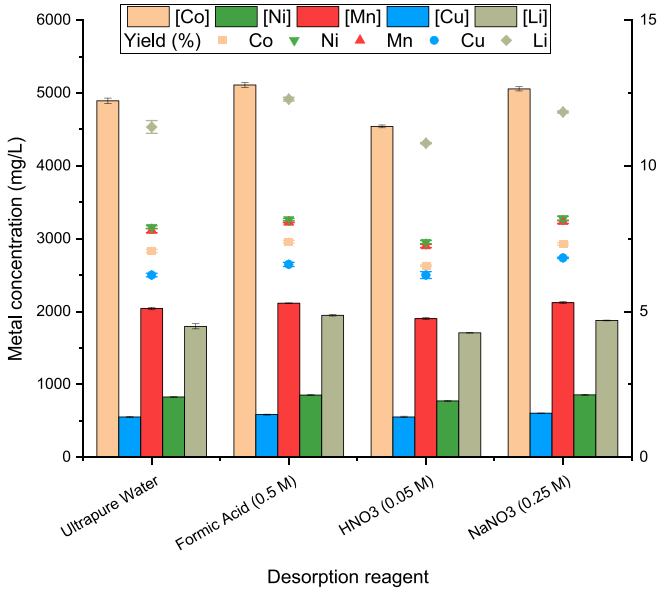


**Fig. 10.** Concentration of metal desorbed from CNFs-15 present in each desorption reagent and desorption yield of each metal from the spent CNFs-15 with BML.

as a desorption reagent to extract Pb, Cu, and Cd from modified-cellulose from sugarcane bagasse, which reached up to 0.9 g/L [66]. In this last-mentioned paper, the dose of regenerating reagent was lower than other cases, which coincides with the technique applied in this study. A remarkable result is that almost none of the attached Al was recovered, which involves that this process could be a way to increase the Al content inside the NC.

Another critical factor is the level of reusability of the material. As an example, Kardam et al. reached noticeable desorption results of Cd(II), Pb(II), and Ni(II) from CNFs with $HNO_3$ (0.5 M). The CNFs were used as sorbents for low-concentrated single metal solutions (25 mg/L) [67]. These authors remarked that even when the desorption yield of each metal was similar in all the four tested cycles (90–99 %), the CNFs sorption capacity dropped drastically after the fourth desorption cycle. As well, a severe decay was observed between the first and the second regeneration cycles with $HNO_3$ (1 M) in the previously mentioned study where succinic acid mercerized nanocellulose was used to treat Zn(II), Ni(II), Co(II) and Cd(II) [36]. The metal sorption capacity after two cycles was 2.8 to 5.4-fold lower than the first one. Ultrasound treatment of the spent nanocelluloses was necessary to reach the full recyclability of the materials after the second regeneration cycle. Considering that in most of the cases, the recyclability and desorption treatments through acids are applied to simple synthetic solutions in most of the cases, and the impact of the difference between the initial metal concentrations of the studies in bibliography and the ones applied in this study, up to several orders of magnitude. Some authors remarked that this reduction in the yield may be caused by the large metal coverage of active sites throughout the NC surface; the continuous degradation of the material after a certain number of desorption batches under low pH conditions; and the presence of impurities covering the active sites. All these three conditions would be expected to play a significant role in the desorption of metals in the treatment of BML with CNCs and CNFs presented in this study. Therefore, the results obtained in a single desorption cycle in this study might be considered as the best ones for metal recovery from spent NCs.

The desorption yield was relatively low in all the cases. This fact is strongly correlated with the metal-NC interaction mechanism described before, including a first sorption and a posterior surface precipitation. As observed in previous studies, the metal recoveries exceeded the cationic demand of the CNFs-15. This means that only the fraction of sorbed metal attached with weaker interactions (through sorption instead of surface precipitation), could be easily extracted from the NCs with the use of the tested solutions. Other studies suggest that the acidic treatment for metal desorption also provides new bonding sites on the spent NCs, which would replace free active sites present in the raw CNFs without freeing the spent active sites [36].

## 4. Conclusions

For the first time, very high selective metal recovery from BML has been obtained using NC as adsorbents. A MSB treatment process has been successfully applied for the recovery of critical metals from BML.

Metal leaching from non-pyrolyzed black mass with HCl presented the highest critical metal extraction yield. Critical metal concentrations ranging between 1 and 10 g/L were obtained in this process. The treatment of MMS revealed a higher selectivity towards Co recovery in batches under pH 1–2 conditions; and larger selectivity for Cu and Ni at pH 4–5. Metal recoveries of 135 g/g were achieved and the selectivity indexes between metals reached values above 40. In the treatment of BML, the metal recoveries were also remarkable, even higher than 30 g/g.

During the MSB treatment, it was observed that a number of batches showed higher selectivity recoveries for certain metals. The process seems to favor Co selectivity over other elements at low pH, but Al (pH 3–4) and Li (CNCs at pH 5) showed the larger selectivity as pH increased. A process to reinforce the Co recovery from BML was successfully tested.

In some steps, where CNC were used, more than 4 g/g of Co could be achieved, achieving more than 99 % total metal recovery.

In the desorption tests, up to 5 g/L of metal could be extracted using any of the tested desorption reagents, which is much higher than previously published results. More than 85 % of the metals recovered remained associated to the CNFs-15. This could be associated with both the low concentration of the desorption reagents ($HNO_3$, formic acid and $NaNO_3$) for the high metal content onto the CNFs-15, and the surface precipitation mechanism.

The results reported in this paper show the significant potential of the implementation of NC materials as an environmentally friendly solution for metal recovery from spent LIBs.

## CRediT authorship contribution statement

**Francisco de Borja Ojembarrena: . Noemi Merayo:** Writing – review & editing, Supervision, Methodology, Formal analysis, Conceptualization. **Angeles Blanco:** Writing – review & editing, Supervision, Resources, Methodology, Conceptualization. **Carlos Negro:** Writing – review & editing, Supervision, Resources, Project administration, Methodology, Funding acquisition, Formal analysis, Conceptualization. **Eric D. van Hullebusch:** Writing – review & editing, Visualization, Validation, Supervision, Resources, Methodology, Investigation, Formal analysis, Conceptualization.

## Declaration of competing interest

The authors declare that they have no known competing financial interests or personal relationships that could have appeared to influence the work reported in this paper.

## Data availability

No data was used for the research described in the article.

## Acknowledgements

The authors are grateful for the financial support by the Ministry of Science and Innovation of Spain (project PID2020-113850RB-C21 “CON-FUTURO”) as well as for the grant provide to F.B. Ojembarrena (PRE2018-085034) for the stay at the Paris Institute of Earth Physics. In addition, Eric D. van Hullebusch (Université Paris Cité and Institut de physique du Globe de Paris) thanks the Horizon 2020 ERA-MIN2 Project Bio-assisted Closed Loop Recycling for E-mobility Metals from waste PCBs and Li-Ion Batteries - BaCLEM (Project ANR-20-MIN2-0002, 2021-2024) for financial support. Eric D. van Hullebusch (Université Paris Cité and Institut de physique du Globe de Paris) thanks government funding managed by the Agence Nationale de la Recherche (French National Research Agency) under the Investissements d’avenir programme under the reference “ANR-21-EXES-0002”.

## Appendix A. Supplementary data

Supplementary data to this article can be found online at https://doi.org/10.1016/j.seppur.2024.126940.

## References

[1] S. Krishnan, N.S. Zulkapli, H. Kamyab, S.M. Taib, M.F.B.M. Din, Z.A. Majid, S. Chaiprapat, I. Kenzo, Y. Ichikawa, M. Nasrullah, S. Chelliapan, N. Othman, Current technologies for recovery of metals from industrial wastes: an overview, Environ. Technol. Innov. 22 (2021) 101525, https://doi.org/10.1016/j.eti.2021.101525.

[2] REGULATION OF THE EUROPEAN PARLIAMENT AND OF THE COUNCIL establishing a framework for ensuring a secure and sustainable supply of critical raw materials and amending Regulations (EU) 168/2013, (EU) 2018/858, 2018/1724 and (EU) 2019/1020, in: E. Parliament (Ed.) EUR-Lex, EUR-Lex, 2023.

[3] Study on the critical raw materials for the EU 2023 – Final report, in: I.E. Directorate-General for Internal Market (Ed.) Publications Office of the European Union, 2023.

[4] J. Burton, U.S Geological Survey Releases 2022 List of Critical Minerals, 2022. https://www.usgs.gov/news/national-news-release/us-geological-survey-releases-2022-list-critical-minerals. (Accessed 13th September 2023.

[5] P. Kowalski, C. Legendre, Raw Materials Critical for the Green Transition (2023), https://doi.org/10.1787/c6bb598b-en.

[6] J.J. Roy, S. Rarotra, V. Krikstolaityte, K.W. Zhuoran, Y.-D.-I. Cindy, X.Y. Tan, M. Carboni, D. Meyer, Q. Yan, M. Srinivasan, Green recycling methods to treat lithium-ion batteries E-waste: a circular approach to sustainability, Adv. Mater. 34 (25) (2022) 2103346, https://doi.org/10.1002/adma.202103346.

[7] D.S. Premathilake, A.B. Botelho Junior, J.A.S. Tenório, D.C.R. Espinosa, M. Vaccari, Designing of a decentralized pretreatment line for EOL-LIBs based on recent literature of LIB recycling for black mass, Metals 13 (2) (2023) 374.

[8] T. Punt, S.M. Bradshaw, P. van Wyk, G. Akdogan, The efficiency of black mass preparation by discharge and alkaline leaching for LIB recycling, Minerals 12 (6) (2022) 753, https://doi.org/10.3390/min12060753.

[9] F. Vasilyev, S. Virolainen, T. Sainio, Numerical simulation of counter-current liquid–liquid extraction for recovering Co, Ni and Li from lithium-ion battery leachates of varying composition, Sep. Purif. Technol. 210 (2019) 530–540, https://doi.org/10.1016/j.seppur.2018.08.036.

[10] G. Patents, Number of patents containing the words (black mass metal recovery), 2023. https://patents.google.com/?q=(black+mass+metal+recovery)&before=priority:20210101&after=priority:20200101. (Accessed 8th December 2023.

[11] D. Latini, M. Vaccari, M. Lagnoni, M. Orefice, F. Mathieux, J. Huisman, L. Tognotti, A. Bertei, A comprehensive review and classification of unit operations with assessment of outputs quality in lithium-ion battery recycling, J. Power Sources 546 (2022) 231979, https://doi.org/10.1016/j.jpowsour.2022.231979.

[12] A. Tuncuk, V. Stazi, A. Akcil, E.Y. Yazici, H. Deveci, Aqueous metal recovery techniques from e-scrap: hydrometallurgy in recycling, Miner. Eng. 25 (1) (2012) 28–37, https://doi.org/10.1016/j.mineng.2011.09.019.

[13] A.B. Botelho Junior, S. Stopic, B. Friedrich, J.A.S. Tenório, D.C.R. Espinosa, Cobalt recovery from Li-ion battery recycling: a critical review, Metals 11 (12) (2021), https://doi.org/10.3390/met11121999.

[14] U. Saleem, B. Joshi, S. Bandyopadhyay, Hydrometallurgical routes to close the loop of electric vehicle (EV) lithium-ion batteries (LIBs) value chain: a review, Journal of Sustainable Metallurgy 9 (3) (2023) 950–971, https://doi.org/10.1007/s40831-023-00718-w.

[15] M. Sethurajan, E.D. van Hullebusch, D. Fontana, A. Akcil, H. Deveci, B. Batinic, J. P. Leal, T.A. Gasche, M. Ali Kucuker, K. Kuchta, I.F.F. Neto, H.M.V.M. Soares, A. Chmielarz, Recent advances on hydrometallurgical recovery of critical and precious elements from end of life electronic wastes - a review, Crit. Rev. Environ. Sci. Technol. 49 (3) (2019) 212–275, https://doi.org/10.1080/10643389.2018.1540760.

[16] J. Neumann, M. Petranikova, M. Meeus, J.D. Gamarra, R. Younesi, M. Winter, S. Nowak, Recycling of lithium-ion batteries—current state of the art, circular economy, and next generation recycling, Adv. Energy Mater. 12 (1C7) (2022) 2102917, https://doi.org/10.1002/aenm.202102917.

[17] M.A. Zazycki, E.H. Tanabe, D.A. Bertuol, G.L. Dotto, Adsorption of valuable metals from leachates of mobile phone wastes using biopolymers and activated carbon, J. Environ. Manage. 188 (2017) 18–25, https://doi.org/10.1016/j.jenvman.2016.11.078.

[18] T.M. Budnyak, S. Modersitzki, I.V. Pylypchuk, J. Piątek, A. Jaworski, O. Sevastyanova, M.E. Lindström, A. Slabon, Tailored hydrophobic/hydrophilic lignin coatings on mesoporous silica for sustainable COBALT(II) recycling, ACS Sustain. Chem. Eng. 8 (43) (2020) 16262–16273, https://doi.org/10.1021/acssuschemeng.0c05696.

[19] J.M. da Cunha, L. Klein, M.M. Bassaco, E.H. Tanabe, D.A. Bertuol, G.L. Dotto, Cobalt recovery from leached solutions of lithium-ion batteries using waste materials as adsorbents, Can. J. Chem. Eng. 93 (12) (2015) 2198–2204, https://doi.org/10.1002/cjce.22331.

[20] S. Ashoka Sahadevan, X. Xiao, Y. Ma, K. Forsberg, R.T. Olsson, J.M. Gardner, Sulfur–oleylamine copolymer synthesized via inverse vulcanization for the selective recovery of copper from lithium-ion battery E-waste, Mater. Chem. Front. 7 (7) (2023) 1374–1384, https://doi.org/10.1039/D2QM01093C.

[21] P. Wamea, M.L. Pitcher, J. Muthami, A. Sheikhi, Nanoengineering cellulose for the selective removal of neodymium: towards sustainable rare earth element recovery, Chem Eng J 428 (2022) 131086, https://doi.org/10.1016/j.cej.2021.131086.

[22] R. Reshmy, E. Philip, A. Madhavan, A. Pugazhendhi, R. Sindhu, R. Sirohi, M. K. Awasthi, A. Pandey, P. Binod, Nanocellulose as green material for remediation of hazardous heavy metal contaminants, J. Hazard. Mater. 424 (2022) 127516, https://doi.org/10.1016/j.jhazmat.2021.127516.

[23] H. Jiang, S. Wu, J. Zhou, Preparation and modification of nanocellulose and its application to heavy metal adsorption: a review, Int J Biol Macromol 236 (2023) 123916, https://doi.org/10.1016/j.ijbiomac.2023.123916.

[24] M.Y. Khalid, A. Al Rashid, Z.U. Arif, W. Ahmed, H. Arshad, Recent advances in nanocellulose-based different biomaterials: types, properties, and emerging applications, J. Mater. Res. Technol. 14 (2021) 2601–2623, https://doi.org/10.1016/j.jmrt.2021.07.128.

[25] R. Reshmy, D. Thomas, E. Philip, S.A. Paul, A. Madhavan, R. Sindhu, P. Binod, A. Pugazhendhi, R. Sirohi, A. Tarafdar, A. Pandey, Potential of nanocellulose for wastewater treatment, Chemosphere 281 (2021), https://doi.org/10.1016/j.chemosphere.2021.130738.

[26] Q. Zhu, Y. Wang, M. Li, K. Liu, C. Hu, K. Yan, G. Sun, D. Wang, Activable carboxylic acid functionalized crystalline nanocellulose/PVA-co-PE composite nanofibrous membrane with enhanced adsorption for heavy metal ions, Sep. Purif. Technol. 186 (2017) 70–77, https://doi.org/10.1016/j.seppur.2017.05.050.
[27] E.I. Unuabonah, G.U. Adie, L.O. Onah, O.G. Adeyemi, Multistage optimization of the adsorption of methylene blue dye onto defatted carica papaya seeds, Chem Eng J 155 (3) (2009) 567–579, https://doi.org/10.1016/j.cej.2009.07.012.
[28] F.d.B. Ojembarrena, E. Fuente, A. Blanco, C. Negro, CR(VI) removal from fiber cement process waters: a techno-economic assessment, Journal of Water Process Engineering 57 (2024) 104594, https://doi.org/10.1016/j.jwpe.2023.104594.
[29] F.d.B. Ojembarrena, J.L. Sánchez-Salvador, S. Mateo, A. Balea, A. Blanco, N. Merayo, C. Negro, Modeling of hexavalent chromium removal with hydrophobically modified cellulose nanofibers, Polymers 14 (16) (2022) 3425, https://doi.org/10.3390/polym14163425.
[30] C. Campano, A. Balea, Á. Blanco, C. Negro, A reproducible method to characterize the bulk morphology of cellulose nanocrystals and nanofibers by transmission electron microscopy, Cellul. 27 (9) (2020) 4871–4887, https://doi.org/10.1007/s10570-020-03138-1.
[31] J.L. Sanchez-Salvador, C. Campano, C. Negro, M.C. Monte, A. Blanco, Increasing the possibilities of TEMPO-mediated oxidation in the production of cellulose nanofibers by reducing the reaction time and reusing the reaction medium, Advanced Sustainable Systems 5 (4) (2021) 2000277, https://doi.org/10.1002/adsu.202000277.
[32] S.Y. Park, S. Goo, H. Shin, J. Kim, H.J. Youn, Structural properties of cellulose nanofibril foam depending on wet foaming conditions in pickering stabilization, Cellul. 28 (16) (2021) 10291–10304, https://doi.org/10.1007/s10570-021-04151-8.
[33] A. Balea, N. Merayo, E. De La Fuente, C. Negro, Á. Blanco, Assessing the influence of refining, bleaching and TEMPO-mediated oxidation on the production of more sustainable cellulose nanofibers and their application as paper additives, Ind. Crop. Prod. 97 (2017) 374–387, https://doi.org/10.1016/j.indcrop.2016.12.050.
[34] F. Serra-Parareda, Q. Tarrés, J.L. Sanchez-Salvador, C. Campano, M.À. Pèlach, P. Mutjé, C. Negro, M. Delgado-Aguilar, Tuning morphology and structure of non-woody nanocellulose: ranging between nanofibers and nanocrystals, Ind. Crop. Prod. 171 (2021) 113877, https://doi.org/10.1016/j.indcrop.2021.113877.
[35] J.L. Sanchez-Salvador, M.C. Monte, W. Batchelor, G. Garnier, C. Negro, A. Blanco, Characterizing highly fibrillated nanocellulose by modifying the gel point methodology, Carbohydr. Polym. 227 (2020) 115340, https://doi.org/10.1016/j.carbpol.2019.115340.
[36] S. Hokkanen, E. Repo, M. Sillanpaa, Removal of heavy metals from aqueous solutions by succinic anhydride modified mercerized nanocellulose, Chem. Eng. J. 223 (2013) 40–47, https://doi.org/10.1016/j.cej.2013.02.054.
[37] T. Saito, A. Isogai, Ion-exchange behavior of carboxylate groups in fibrous cellulose oxidized by the TEMPO-mediated system, Carbohydr. Polym. 61 (2) (2005) 183–190, https://doi.org/10.1016/j.carbpol.2005.04.009.
[38] S. Srivastava, A. Kardam, K.R. Raj, Nanotech reinforcement onto cellulosic fibers: green remediation of toxic metals, Int. J. Green Nanotechnol. 4 (1) (2012) 46–53, https://doi.org/10.1080/19430892.2012.654744.
[39] L. Brückner, J. Frank, T. Elwert, Industrial recycling of lithium-ion batteries—a critical review of metallurgical process routes, Metals 10 (8) (2020) 1107, https://doi.org/10.3390/met10081107.
[40] S.D. Widijatmoko, F. Gu, Z. Wang, P. Hall, Selective liberation in dry milled spent lithium-ion batteries, Sustain. Mater. Technol. 23 (2020) e00134.
[41] P. Meshram, B.D. Pandey, T.R. Mankhand, Recovery of valuable metals from cathodic active material of spent lithium ion batteries: leaching and kinetic aspects, Waste Manag. 45 (2015) 306–313, https://doi.org/10.1016/j.wasman.2015.05.027.
[42] I. Balázs Illés, T. Kékesi, Extraction of pure Co, Ni, Mn, and Fe compounds from spent Li-ion batteries by reductive leaching and combined oxidative precipitation in chloride media, Miner. Eng. 201 (2023) 108169, https://doi.org/10.1016/j.mineng.2023.108169.
[43] J. Partinen, P. Halli, B.P. Wilson, M. Lundström, The impact of chlorides on NMC leaching in hydrometallurgical battery recycling, Miner. Eng. 202 (2023) 108244, https://doi.org/10.1016/j.mineng.2023.108244.
[44] C. Liu, J. Long, Y. Gao, H. Liu, W. Luo, X. Wang, Microwave low-temperature treatment – step leaching process for recovering black mass from spent lithium-ion batteries, J Environ Chem Eng 11 (3) (2023) 109759, https://doi.org/10.1016/j.jece.2023.109759.
[45] P.A.P. Silva, R.L. Oréfice, Bio-sorbent from Castor oil polyurethane foam containing cellulose-halloysite nanocomposite for removal of manganese, nickel and cobalt ions from water, J. Hazard. Mater. 454 (2023) 131433, https://doi.org/10.1016/j.jhazmat.2023.131433.
[46] X. Li, Y. Tang, X. Cao, D. Lu, F. Luo, W. Shao, Preparation and evaluation of orange peel cellulose adsorbents for effective removal of cadmium, zinc, cobalt and nickel, Colloids Surf A Physicochem Eng Asp 317 (1) (2008) 512–521, https://doi.org/10.1016/j.colsurfa.2007.11.031.
[47] S. Hokkanen, E. Repo, T. Suopajärvi, H. Liimatainen, J. Niinimaa, M. Sillanpää, Adsorption of NI(II), CU(II) and CD(II) from aqueous solutions by amino modified nanostructured microfibrillated cellulose, Cellul. 21 (3) (2014) 1471–1487, https://doi.org/10.1007/s10570-014-0240-4.
[48] N. Conte, J.M. Gómez, Improving the sorption properties of mesoporous carbons for the removal of cobalt, nickel and manganese from spent lithium-ion batteries effluent, Sep. Purif. Technol. 328 (2024) 125095, https://doi.org/10.1016/j.seppur.2023.125095.
[49] J.S.R. Fernando, Selective Recovery of Nickel and Cobalt from Spent Battery Waste (Black Mass) by Adsorption: Resin and MOF Case Study, Department of Chemistry, Bioscience and Environmental Engineering University of Stavanger, https://uis.brage.unit.no/uis-xmlui/handle/11250/3022619, 2022, p. 134.
[50] M.L. Strauss, L.A. Diaz, J. McNally, J. Klaehn, T.E. Lister, Separation of cobalt, nickel, and manganese in leach solutions of waste lithium-ion batteries using dowex M4195 ion exchange resin, Hydrometall. 206 (2021) 105757, https://doi.org/10.1016/j.hydromet.2021.105757.
[51] Membrane filtration: Managing aluminum in membrane filtration, Filtration + Separation 51(4) (2014) 26-28. 10.1016/S0015-1882(14)70145-4.
[52] X. Shen, G. Qiu, C. Yue, M. Guo, M. Zhang, Multiple copper adsorption and regeneration by zeolite 4A synthesized from bauxite tailings, Environ Sci Pollut R 24 (27) (2017) 21829–21835, https://doi.org/10.1007/s11356-017-9824-5.
[53] S. Hokkanen, A. Bhatnagar, V. Srivastava, V. Suorsa, M. Sillanpaa, Removal of Cd2+, Ni2+ and PO43- from aqueous solution by hydroxyapatite-bentonite clay-nanocellulose composite, Int J Biol Macromol 118 (2018) 903–912, https://doi.org/10.1016/j.ijbiomac.2018.06.095.
[54] H. Şahan, H. Göktepe, Ş. Patat, S. Yıldız, B. Özdemir, A. Ülgen, S. Mukerjee, K. M. Abraham, Effect of silver coating on electrochemical performance of 0.5Li2MnO3.0.5 LiMn1/3Ni1/3Co1/3O2 cathode material for lithium-ion batteries, J. Solid State Electrochem. 23 (5) (2019) 1593–1604, https://doi.org/10.1007/s10008-019-04240-6.
[55] Millipore Sigma website. “Dowex” products search., 2024. https://www.sigmaaldrich.com/US/en/search/dowex?focus=products&page=1&perpage=30&sort=relevance&term=dowex&type=product. (Accessed 23th January 2024).
[56] Latin American Pulp, Paper and Forest Products – Peer Review, 2022. https://www.fitchratings.com/research/corporate-finance/latin-american-pulp-paper-forest-products-peer-review-09-11-2022-1#:~:text=Fitch%20Ratings%20forecasts%20bleached%20eucalyptus,USD470%2Fton%20in%20July%202020.. (Accessed 23rd January 2024).
[57] Statistics. THE COTLOOK A INDEX. https://icac.shinyapps.io/ICAC_Open_Data_Dashboaard/#. (Accessed 23rd January 2024).
[58] K. Hughes, Recent Developments in the Global Cotton Market. Cotton By-Products, in: I.C.A. Committee (Ed.) World Trade Organization, https://www.wto.org/english/tratop_e/agric_e/item_3_icac_wto_cotton_by_products_june_2019_final.pdf, 2019, p. 28.
[59] L. Zhang, X. Jia, Y. Ai, R. Huang, W. Qi, Z. He, J.J. Klemeš, R. Su, Greener production of cellulose nanocrystals: an optimised design and life cycle assessment, J. Clean. Prod. 345 (2022) 131073, https://doi.org/10.1016/j.jclepro.2022.131073.
[60] S. Chen, N. Yue, M. Cui, A. Penkova, R. Huang, W. Qi, Z. He, R. Su, Integrating direct reuse and extraction recovery of TEMPO for production of cellulose nanofibrils, Carbohydr. Polym. 294 (2022) 119803, https://doi.org/10.1016/j.carbpol.2022.119803.
[61] H. Xu, J.L. Sanchez-Salvador, A. Blanco, A. Balea, C. Negro, Recycling of TEMPO-mediated oxidation medium and its effect on nanocellulose properties, Carbohydr. Polym. 319 (2023) 121168, https://doi.org/10.1016/j.carbpol.2023.121168.
[62] P. Meshram, S. Virolainen, T.S. Abhilash, Solvent extraction for separation of 99.9% pure cobalt and recovery of Li, Ni, Fe, Cu, Al from Spent LIBs, Metals 12 (6) (2022) 1056.
[63] S. Pavón, D. Kaiser, M. Bertau, Recovery of Al Co, Cu, Fe, Mn, and Ni from spent LIBs after Li selective separation by COOL-process – part 2: solvent extraction from sulphate leaching solution, Chem. Ing. Tech. 93 (11) (2021) 1840–1850, https://doi.org/10.1002/cite.202100101.
[64] N. Vieceli, T. Ottink, S. Stopic, C. Dertmann, T. Swiontek, C. Vonderstein, R. Sojka, N. Reinhardt, C. Ekberg, B. Friedrich, M. Petranikova, Solvent extraction of cobalt from spent lithium-ion batteries: dynamic optimization of the number of extraction stages using factorial design of experiments and response surface methodology, Sep. Purif. Technol. 307 (2023) 122793, https://doi.org/10.1016/j.seppur.2022.122793.
[65] F. Chai, R. Wang, L. Yan, G. Li, Y. Cai, C. Xi, Facile fabrication of pH-sensitive nanoparticles based on nanocellulose for fast and efficient As(v) removal, Carbohydr. Polym. 245 (2020) 116511, https://doi.org/10.1016/j.carbpol.2020.116511.
[66] W. Kong, J. Ren, S. Wang, Q. Chen, Removal of heavy metals from aqueous solutions using acrylic-modified sugarcane bagasse-based adsorbents: equilibrium and kinetic studies, BioResources 9 (2) (2014) 3184–3196, https://doi.org/10.15376/biores.9.2.3184-3196.
[67] A. Kardam, K.R. Raj, S. Srivastava, M.M. Srivastava, Nanocellulose fibers for biosorption of cadmium, nickel, and Lead ions from aqueous solution, Clean Technol. Environ. Policy 16 (2) (2014) 385–393, https://doi.org/10.1007/s10098-013-0634-2.